JMEPEG (2011) 20:382–389
DOI: 10.1007/s11665-010-9687-0

1059-9495/$19.00

Load Ratio Estimation Through Striation Height and Spacing Analysis of an Aerospace Al Alloy 7475-T7351

C.O.F.T. Ruckert, A.A. Messias Filho, W.W. Bose Filho, D. Spinelli, and J.R. Tarpani

(Submitted August 23, 2006; in revised form May 3, 2010)

It is well known that striation spacing may be related to the crack growth rate, d*a*/d*N*, through Paris equation, as well as the maximum and minimum loads under service loading conditions. These loads define the load ratio, *R*, and are considered impossible to be evaluated from the inter-spacing striations analysis. In this way, this study discusses the methodology proposed by Furukawa to evaluate the maximum and minimum loads based on the experimental fact that the relative height of a striation, *H*, and the striation spacing, *s*, are strongly influenced by the load ratio, *R*. Fatigue tests in C(T) specimens were conducted on SAE 7475-T7351 Al alloy plates at room temperature and the results showed a straightforward correlation between the parameters *H*, *s*, and *R*. Measurements of striation height, *H*, were performed using scanning electron microscopy and field emission gun (FEG) after sectioning the specimen at a large inclined angle to amplify the height of the striations. The results showed that for increasing *R* the values of *H*/*s* tend to increase. Striation height, striation spacing, and load ratio correlations were obtained, which allows one to estimate service loadings from fatigue fracture surface survey.

Keywords aerospace, aluminum, electron microscopy, failure analysis

1. Introduction

New aeronautical grade light alloys with improved combination of specific mechanical properties (i.e., high strength and stiffness/weight ratios) are in constant development to improve structural efficiency and save structural weight in commercial aircrafts. Failure in structural aircraft components generally occurs due to cyclic loading (fatigue), which accounts for nearly 80% of total investigated cases (Ref 1, 2).

Analyzing the striation pattern in the wake of sub-critical crack propagation often allows the determination of fatigue crack growth rates in function of crack size (length and/or depth). Nevertheless, the inspection of the fracture surface is not enough to derive load levels that effectively caused crack advance. In this sense, d*a*/d*N* curves obtained from constant amplitude loading (CAL) fatigue testing still provide essential data for the characterization of the striation pattern of the material, as well as information on the fatigue crack propagation rate that are indispensable to load predictions.

It is known that the striation spacing, *s*, and the crack growth rate, d*a*/d*N*, are coincident at the Paris region for load ratio $R = 0.1$. The counting of striations was suggested many years ago as a method to estimate the crack growth rate. Several authors claim a one-to-one correspondence between striation length and stress cycle (Ref 3, 4). However, other authors found that there is no simple correlation between striations and stress cycles. According to Broek (Ref 3) and more recently to Nedbal (Ref 4), the 1:1 correlation between the microscopic, *s*, and the macroscopic, d*a*/d*N*, crack growth rates is valid only within the fatigue crack growth rate range of 0.1, to 1 μm/cycle for aluminum alloys and up to 70 μm/cycle in a ductile structural steel (Ref 5). For aluminum alloys, above this range d*a*/d*N* is increased due to monotonic fracture modes intercepting fatigue crack growth, so that microvoid nucleation and/or local cleavage triggered in the vicinity of intermetallic particles control crack advancing. Below this range, *s* is larger than d*a*/d*N* due to the irregularities of the crack front and/or idle load

C.O.F.T. Ruckert, A.A. Messias Filho, W.W. Bose Filho, D. Spinelli, and **J.R. Tarpani**, Materials, Aeronautics and Automotive Engineering Department, Engineering School of São Carlos, University of São Paulo, São Carlos, SP 13566-590, Brazil Contact e-mail: cassius@sc.usp.br.

List of symbols

d*a*/d*N*	Crack growth rate
s	Striation spacing
K_{max}	Maximum applied stress intensity factor
R	Applied stress ratio
Δ*K*	Applied stress intensity factor range
S_u	Tensile strength
S_{ys}	0.2% offset yield strength
E	Young's modulus
RA	Reduction of area
Δ*L*	Elongation at 25 mm (gauge length)
C(T)	Compact tension specimen
H	Striation height measure corrected by the cutting surface
h	Height measured in the image obtained by FEG
α	Cutting angle
H/*s*	Morphologic striation ratio (dimensionless)
Δ_{ai}	Striation spacing distance measurement at the fracture surface
P_{max}	Maximum service load
P_{min}	Minimum service load

cycles, which do not result in effective crack growth. Because the relationship between da/dN, s, and ΔK (stress intensity factor range = $K_{max} - K_{min}$) or ΔK_{eff} (effective stress intensity factor range) satisfies Paris'law, attempts have been made to estimate the service load from the striation spacing (s) on the fracture surface (Ref 6, 7).

In this study, Furukawa's methodology (Ref 6, 7) to determine the fatigue load ratio, R, relying in experimental measurements of striation spacing, s, and striation height, h, is assessed for an advanced aeronautical grade Al alloy. The results corroborated the validity of this technique, enabling one to estimate the load rates applied in-test or in-service conditions, so that the minimum load to cause sub-critical crack growth can be properly inferred.

What is important here, then, is whether the stress ratio R can be determined from the configuration and dimensions of the striations.

2. Material Tested

7475 Al-alloy, thermomechanically treated for T7351 condition (Ref 8) has been tested. When subjected to fatigue loads, the high ductility of the alloy was responsible for the generation of well-defined and clearly observed striation marks over the fracture surface. Table 1 and 2 presents, respectively, tensile properties and chemical composition of the Al 7475-T7351 alloy. The microstructure of the aluminium alloy is showed in Fig. 1. Texture is found in the rolling direction, L. Wide nonrecrystallized regions and segregation can be observed in LS, and particularly, in TS planes.

3. Experimental Procedure

Two types of crack growth rate experiments were used:

(i) constant ΔK and R, to analyze the striation morphology H/s and
(ii) crack growth rate with increasing ΔK, for the da/dN vs. ΔK curve.

On the experiments accomplished with constant ΔK and increasing R (0.1, 0.3, 0.5, and 0.7), four compact tension specimens, C(T), were used. They were fabricated with LT orientation parallel to crack direction and geometry and dimensions as presented in Fig. 2. In these specimens, three distinct ΔK levels were applied in a stepwise manner, to allow further reading of striation spacing at constant-ΔK locations, as schematically depicted in Fig. 3.

For sample cutting, a novel technique based on the previous study of Furakawa (Ref 7) was used. After testing, the fracture surfaces were protected with Technovit 5071 resin, to avoid striation damage (border effect) at the cutting operation, as shown in Fig. 4. One fracture side of each test specimen was cut at an angle of approximately 30° to 34° using a silicon

Table 1 Tensile properties of the tested Al-alloy in longitudinal (lamination) direction

S_{ys} (0.2%), MPa	S_u, MPa	E, GPa	ΔL, %	RA, %
395	470	71.4	16.6	19.4

Table 2 Chemical composition of SAE AMS 7475-T7351 Al alloy (wt.%)

Si	Fe	Cu	Mg	Cr	Ni	Zn	P	Zr
0.05	0.07	1.76	1.95	0.24	0.01	5.79	0.01	0.12

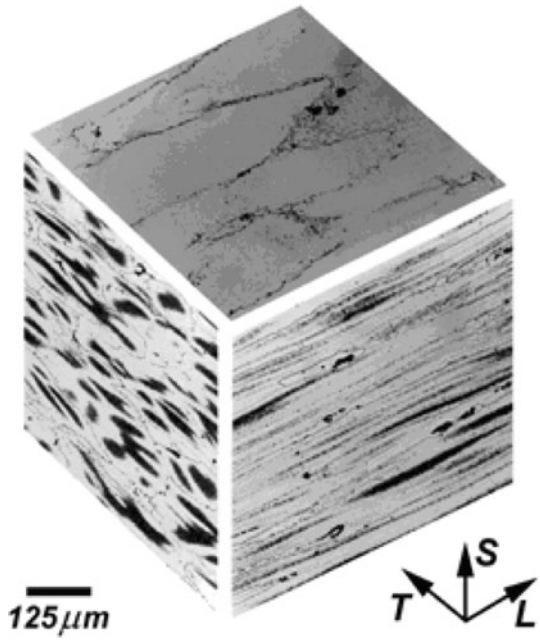

Fig. 1 Tri-dimensional view of the microstructure of the studied aluminium alloy

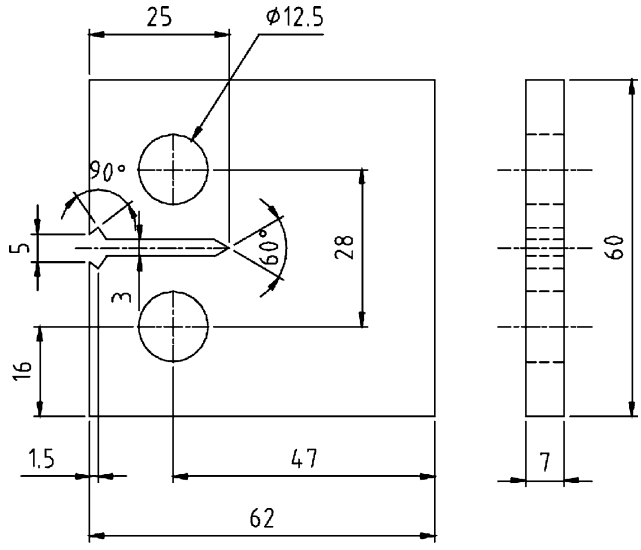

Fig. 2 Geometry and dimensions of C(T) specimens for crack propagation tests performed at constant ΔK and increasing R according to ASTM-E647-05 (dimensions in mm)

carbide disk at 3000 rpm, constant load of 300 g, and a coolant. These operations have to be done to magnify and facilitate the measurement of the striations' height.

Following, the resin was removed from the fracture surface using acetone, which has no harmful action on the aluminum alloy fracture surface. Striation spacing, s, and the striation height, H, were observed and photographed in a scanning electron microscope, using magnifications ranging from 5000 to 20,000× (SEM) and 5000 to 100,000× (FEG-VP SUPRA-35 ZEISS). The former were used to measure the height and striation spacing at lower levels of ΔK. Figure 5 shows the image acquisition scheme in field emission gun (FEG) and SEM. Note that the first striation spacing was taken longitudinally at 2.5 mm ahead of the fatigue precrack tip and the others at each 5 mm. Transversely, the measurements were taken at each 1.4 mm alongside the test specimen thickness. At each increment of crack size, Δ_{ai}, five photographs were taken, the measurements of H and s were performed and a mean value of these five measurements was calculated.

The measurements of striation spacing, s, and height were carried out using a digital image analyzer showed in Fig. 6.

Figure 7 shows schematically the methodology of height H measurement using the image obtained from the FEG microscope. The measures of the striations height, h, were corrected due to the cutting angle, according to Eq 1.

$$H = h * \cos\alpha \qquad \text{(Eq 1)}$$

where h is the measure of height in the image obtained by FEG; H is the measure of height corrected by the cutting angle; α is the cutting angle (from 30° to 34°) of the fracture surface.

Estimating R from H/s and measuring the crack growth rate from s, ΔK can be determined and the service loading can be evaluated.

Table 3 illustrates the flow chart for the above-mentioned procedure for the determination of service loadings from fatigue fracture surface.

4. Results and Discussions

Figure 8 shows the crack growth rate curve, da/dN, the striation spacing, s and ΔK for the specimens tested at increasing stress intensity factor, ΔK. The compliance technique was

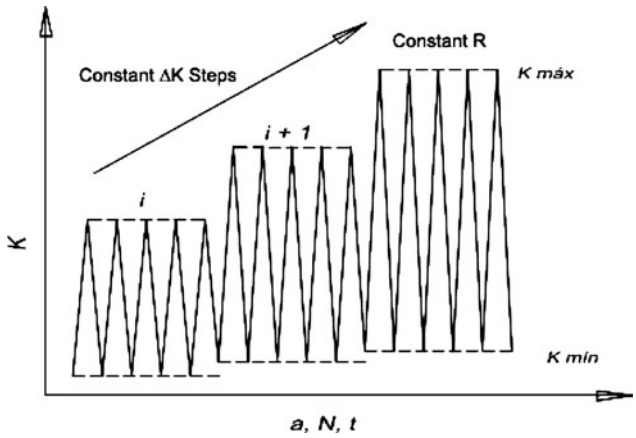

Fig. 3 Applied loading spectrum in terms of K-stress intensity factor

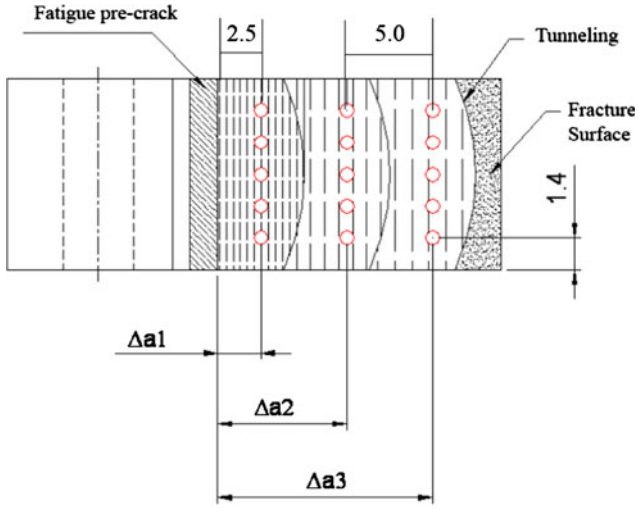

Fig. 5 Sketch showing how the striation spacing (s) on the fracture surface of C(T) test specimens were measured (distances in mm)

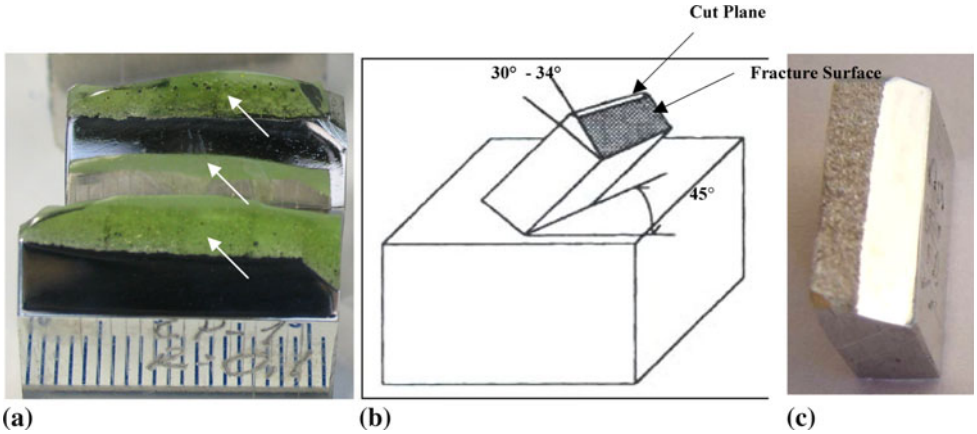

Fig. 4 (a) Test specimens with the fracture surface protected by resin Technovit 5071, showed by *arrows*, (b) schematic showing the cutting plane and fracture surface, (c) fracture surface after resin removed

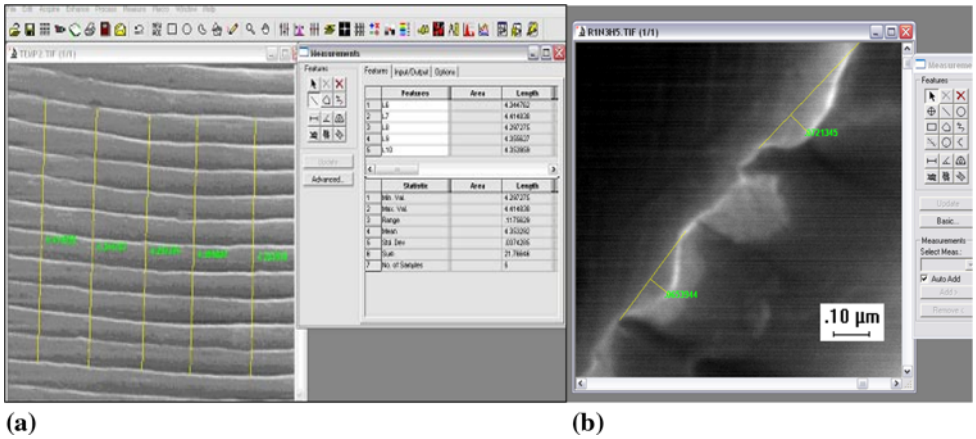

Fig. 6 Digital image analyzer used to measurement (a) striation spacing, *s* and (b) height striation, *h*

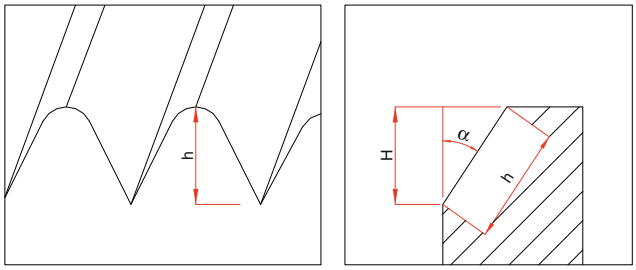

Fig. 7 Scheme of striation height *H* measurement from FEG images

Table 3 Flowchart for determination of service loading (Ref 6)

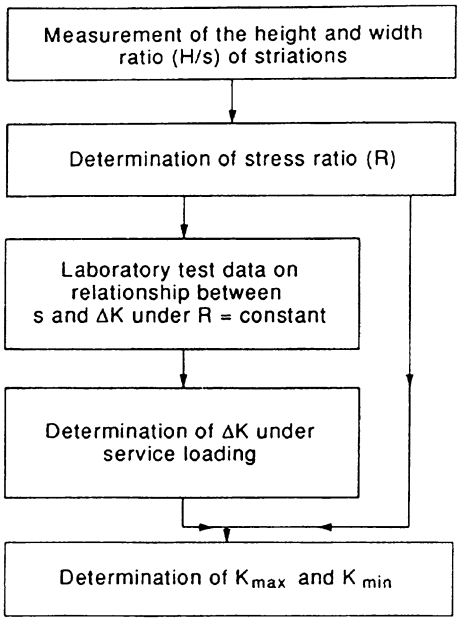

employed to measure crack size and the striation spacing, *s*, was measured using SEM and FEG. It is noticed that only the data corresponding to Paris region were presented in the

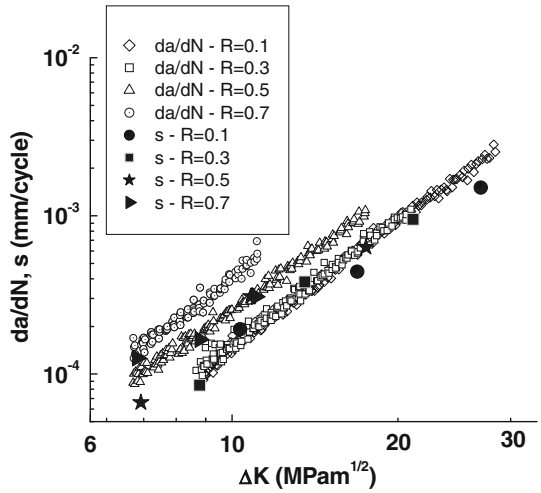

Fig. 8 The figure shows Δ*K*, d*a*/d*N* and the striation spacing, *s* for the four load ratio, *R*, applied during the tests

graphic. From this figure, it is possible to see that the crack growth rate is influenced not only by Δ*K* but also by *R*. There is no 1:1 (one-to-one) correspondence between the crack growth rate and *s* with the increasing *R*, therefore the error of the correlation increases with increase of *R* and Δ*K*. However, to determine service loadings from fracture surface, not only crack growth rate (d*a*/d*N* or *s*) but also load ratio, *R* must be determined from the fracture surface.

Figure 9 shows images of striation sections observed in FEG microscope for various stress ratios, *R* and Δ*K*, demonstrating the large range of the *H*/*s* distribution for each stress ratio *R* and the stress intensity factor, Δ*K* for the 7475-T351 Al alloy. It can be seen from Fig. 9(a), (d), and (f) and Table 4, for a Δ*K* almost constant, as *R* increases, both *s* and *H* increases. However, *H* is much more sensitive than *s*, to *R* variation. This suggests that not only stress amplitude but also stress ratio could be obtained by fracture surface analysis. Considering now a constant value of *R*, it is possible to conclude that both *s* and *H* are equally sensitive to changes in Δ*K*; therefore, the ratio *H*/*s* is kept almost constant and independent of K_{max}. The observed nonlinearity occurred possibly due to striation damage (border effect) in the cutting operation. Figure 10 gives further information about the effect of K_{max} on the *H*/*s* ratio.

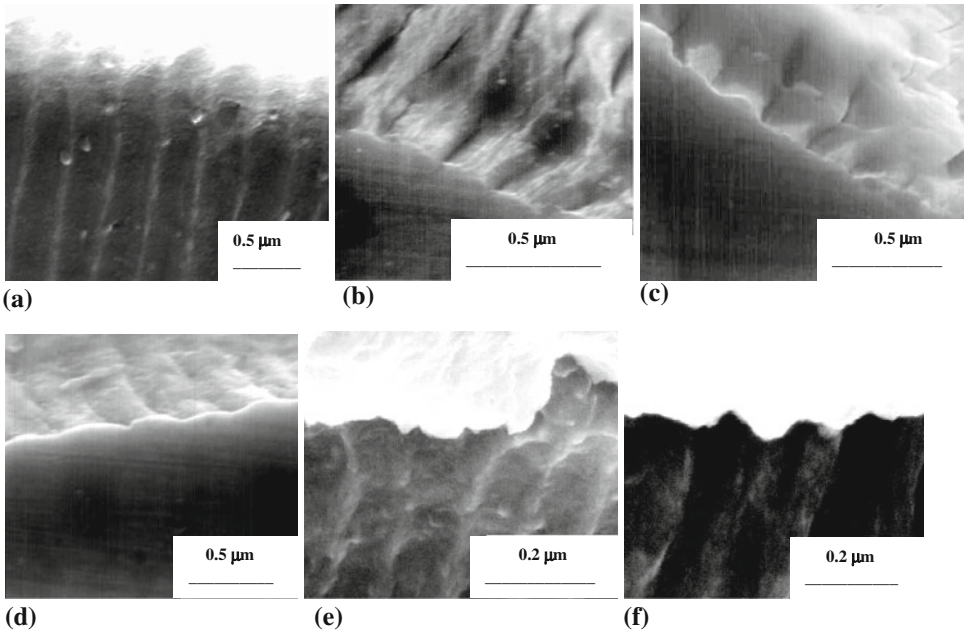

Fig. 9 Striations of the fatigue fractographic surface of SAE 7475-T7351 aluminum alloy which evidence the striations spacing, *s*, and the striations height, *H*, in cut specimens. (a) $R = 0.1$, $\Delta K = 10.3$ MPa·m$^{1/2}$; (b) $R = 0.1$, $\Delta K = 25.0$ MPa·m$^{1/2}$; (c) $R = 0.3$, $\Delta K = 19.2$ MPa·m$^{1/2}$; (d) $R = 0.5$, $\Delta K = 10.7$ MPa·m$^{1/2}$; (e) $R = 0.5$, $\Delta K = 7.2$ MPa·m$^{1/2}$; (f) $R = 0.7$, $\Delta K = 10.9$ MPa·m$^{1/2}$

Table 4 Results of fractographic analyses, corrected height, *H*, and the morphologic striation ratio, *H*/*s*

Load Ratio	ΔK applied, MPa·m$^{1/2}$	Striation spacing, *s*, μm	SD, striation spacing	Height of striation, *H*, μm	SD, height spacing	Morphologic ratio, *H*/*s*, −
0.1	10.2	0.190	0.05	0.038	0.011	0.199
	15.7	0.444	0.08	0.079	0.008	0.179
	25.0	1.507	0.10	0.267	0.090	0.177
0.3	8.9	0.085	0.01	0.018	0.007	0.205
	13.0	0.382	0.07	0.075	0.012	0.196
	19.2	0.950	0.06	0.202	0.086	0.213
0.5	7.2	0.066	0.02	0.019	0.009	0.284
	10.7	0.286	0.05	0.076	0.010	0.266
	16.2	0.633	0.09	0.164	0.067	0.259
0.7	7.1	0.126	0.03	0.046	0.007	0.363
	8.9	0.165	0.04	0.055	0.003	0.333
	10.9	0.308	0.06	0.109	0.078	0.353

SD, standard deviation

Table 4 presents the average values of the results obtained for the corrected height, *H*, and the ratio between height and spacing (*H*/*s*) for the four load ratio levels applied.

The influence of the maximum stress intensity factor (K_{max}) on the (*H*/*s*) ratio for the 7475-T7351 aluminum alloy for distinct values of *R* is shown in Fig. 10. These values appeared to be approximately constant for increasing K_{max}. However, this trend does not occur with respect to the *R* values observed in Fig. 11, in accordance with the study of Furukawa (Ref 6).

It is also understood from Fig. 10 and 11 that the value of *H*/*s* in uniquely determined by *R*, regardless the variation of crack growth rate. By estimating *R* from *H*/*s* and measuring the microscopic crack growth rate *s*, ΔK can be determined, as well as in the service loading.

The mechanism of formation of fatigue striations has been discussed by several researchers (Ref 7, 9, 10). Following the explanations presented by Furukawa et al. (Ref 7), there are minor differences in the hypotheses assumed by these researchers because the slip-off mechanism is the fundamental aspect commonly considered in these hypotheses. The experimental observations in this study seem to be consistent with the slip-off mechanism, if the values of *H*/*s* considered are always smaller than 1.0 and decrease with decreasing *R*, indicating the flattening mechanism of a striation due to crack closure. The measurements in this study show that a scatter of the ratio *H*/*s* even in the group of neighboring striations is presumably caused by the existence of grain boundaries and inhomogeneities, and accordingly the complete slip-off mechanism could not act.

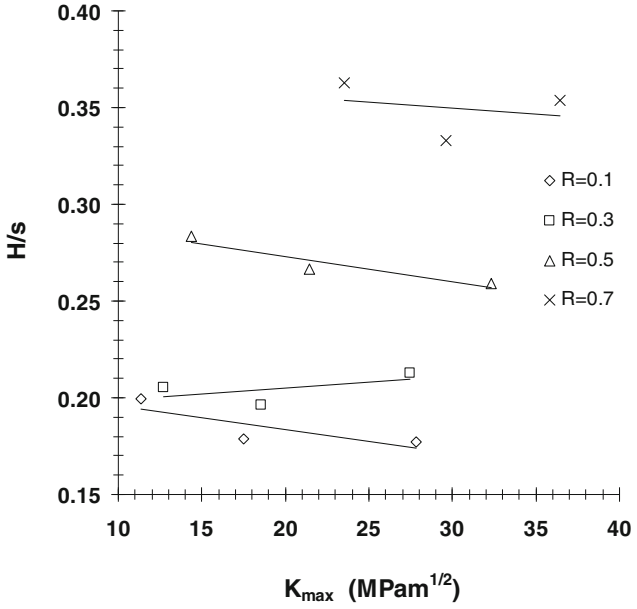

Fig. 10 Influence of the maximum stress intensity factor (K_{max}) on the ratio between striation height H and spacing s (H/s) for the 7475-T7351 aluminum alloy for distinct R

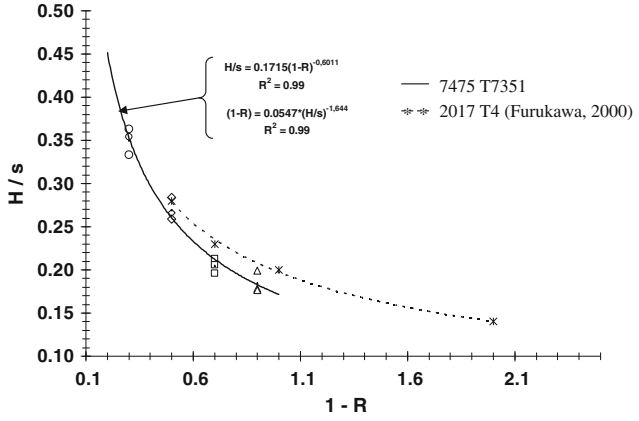

Fig. 11 Relationship between stress ratio R and H/s (H = striation height and s = width ratio) obtained by the SAE 7475-T7351 (continuous line) and 2017-T4 (4, 7) (*dotted line*)

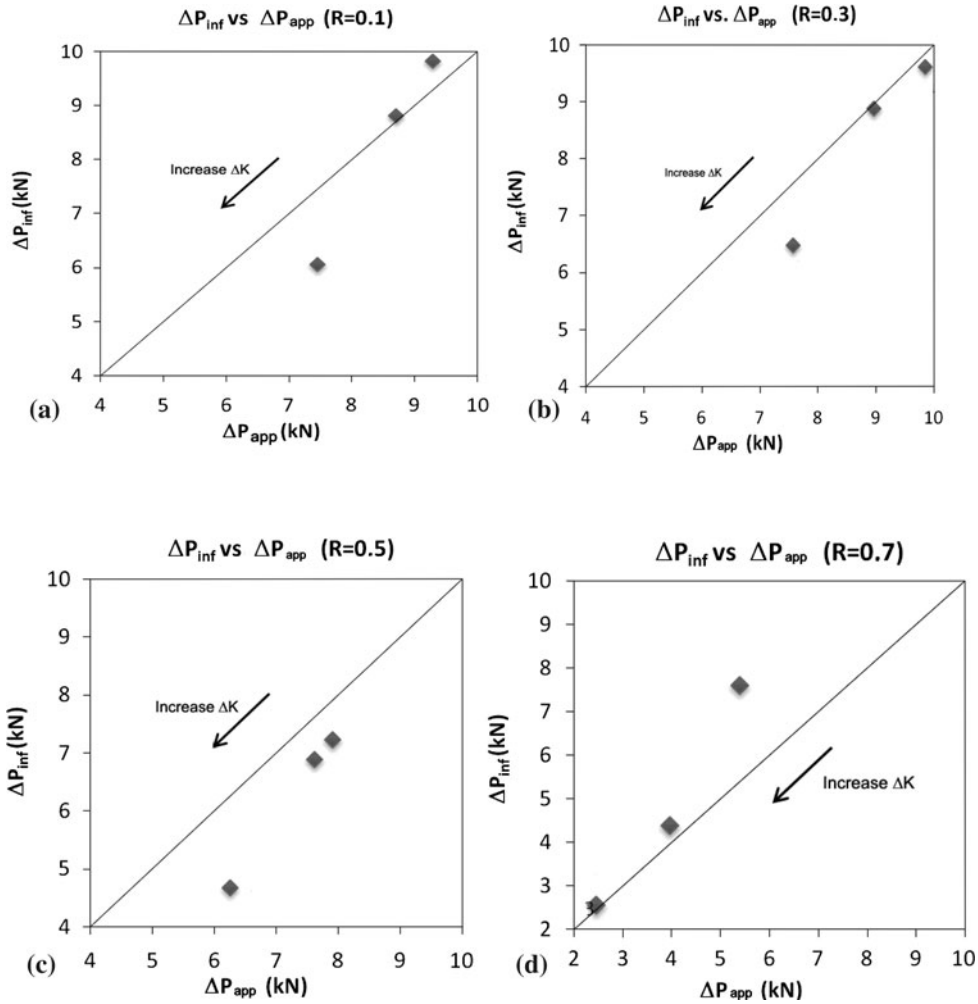

Fig. 12 Direct comparing between the inferred and the applied load to the load ratios (a) 0.1, (b) 0.3, (c) 0.5, and (d) 0.7

Table 5 Predicted load calculated analytically and measured fractographycally, as well as the load estimated error

Load ratio, R	s, μm/cycle	ΔK_{app}, MPa · m^{½}	ΔK_{inf}, MPa · m^{½}	ΔP_{app}, kN	ΔP_{inf}, kN	Error (a), %
0.1	0.190	10.2	10.78	9.29	9.83	5.81
	0.444	15.7	14.27	8.70	8.81	1.26
	1.507	25.0	21.39	7.46	6.06	18.77
0.3	0.085	8.9	8.21	9.85	9.62	2.34
	0.382	13.0	13.41	8.97	8.88	1.00
	0.950	19.2	18.06	7.57	6.48	14.39
0.5	0.066	7.2	6.25	7.91	7.23	8.59
	0.286	10.7	10.40	7.62	6.88	9.71
	0.633	16.2	13.71	6.25	4.68	25.12
0.7	0.126	7.1	6.85	5.40	7.61	40.92
	0.165	8.9	7.48	3.96	4.38	10.61
	0.308	10.9	9.18	2.46	2.56	4.07

(a) Relative error between inferred and applied load, i.e., ΔP_{inf} and ΔP_{app}

Figure 11 shows the relationship between the load ratio R and the striation morphology, H/s (striation height and striations spacing ratio). In the same figure was plotted the results obtained for Furukawa et al. (Ref 6, 7, 9) for the 2017-T4 alloy for comparison purpose. Both the results suggest that the relationship between H/s and R does not vary with the materials. This conclusion has considerable significance and practical importance in estimating the service load from fatigue fracture surfaces.

The scatter band of the values of H/s is large and seems to be inherent in fatigue fracture surface of polycrystalline materials, because this scatter may be caused not only by the locally varying R, but also by crystallographic orientation of grains ahead of the crack tip (Ref 6, 9). The measurement of H/s on several striations enables us to determine the value of R with accuracy suitable for practical purposes.

Figure 12 presents straight correlation between applied and inferred load obtained by the experimental-analytical method. It is observed an increase in the relative error as ΔK increases, exception in the case of $R = 0.7$. Table 5 and Fig. 12 indicate that as R increases the difference between the applied and the inferred loads also increases.

It should be noticed that striation size is quite difficult to measure and the cutting and the polishing method presented here, may bring some difficulties during the striation measurement and only a few valid values can be obtained. The fact is that the fracture surface (even considering the protection enhanced by the resin layer) is easily damaged during the cutting process. Another methodology has been presented by Furukawa (Ref 9) using a Laser microscope, which unfortunately was not available during this analysis. This new method (Ref 9), therefore, offers a way to measure striation height and width more accurately and easily without errors of mechanical cutting using a microtome. Therefore, these errors of correlations may be explained due to increase of ratio H/s of the striations with increasing R, i.e., H is much more sensitive to R variation than s and may be responsible for the non-one-to-one correlation between da/dN and s. Another effect was presented by Broek (Ref 3), who studying two different Al alloys found that above 1 μm/cycle, da/dN is accelerated by ductile tear induced by intermetallic particles, while below 0.1 μm/cycle, s becomes larger than da/dN, due to inhomogeneous extension along the crack front. Thus, further studies are necessary to build up a striation formation mechanism which takes into account the results described above.

The inferred load was determined by the equation relating ΔP and ΔK for 1C(T) geometry described in the ASTM E647 Standard. For this, crack sizes were measured in the obtained images for each load ratio.

The low values of the calculated errors of loading inferences are shown in Table 5, and a tendency in error increases as loading rate and stress intensity factor also increase, with the exception of $R = 0.7$. It is ease to note in Table 5 that the inferred stress intensity factors are close to the applied values. The error in da/dN related to striation spacing, s, in Fig. 8, is not in agreement with the errors in ΔP_{app} and ΔP_{inf}, depicted in Fig. 12 and calculated in Table 5, which could be resulted from the errors in crack length measured in the fracture surface. Furthermore, statistical analyses of morphological striation measurements are necessary.

Table 5 shows the predicted loads analytically calculated (ΔP_{app}) and determined by fractographic techniques (ΔP_{inf}), as well as the load estimate errors after the postmortem analysis. With this statistical analysis the accuracy of the method could be assessed.

5. Conclusion

In this study, fatigue tests were performed in SAE AMS 7475 T7351 Al alloy specimens for several combinations of load ratio R and different stress intensity factor levels, ΔK. The aim was to establish a method for load evaluation from detailed fractographic analysis, using the correlation between the macroscopic crack growth rate, da/dN, and the microscopic propagation, i.e., the striation spacing, s, the variation of stress intensity factor, ΔK, and the inference of the load ratio, R. The following conclusions are listed below:

- In this work it was observed that the striation spacing, s progressively decreases with the decrease of stress intensity factor variation.
- It was seen that striation spacing, s, correlates directly with da/dN only in the interval 0.1-1.0 μm/cycle to $R = 0.1$. For other values, significant divergences of values are found.

The error in the correlation increases as R increases and may be explained due to the changes in morphology (H/s) of the striations with increasing R. H is much more sensitive to R variation than s and may be responsible for the non-one-to-one correlation between da/dN and s. Thus, further studies are necessary to develop a striation formation mechanism which takes into account the results described above.

- It was also observed that H/s values appeared to be approximately constant for increasing K_{max} for the 7475-T7351 alloy. This behavior does not occur in respect to R values, in accordance with the study of Furukawa.
- The experimental methodology used proved to be effective in protecting the striations against damage during cutting, and as the resin is soluble in acetone, it was quite easy to get ride of it without damaging the fracture surface, minimizing error measurements.
- This method indicates the importance of accurate measurement of striation height H in the determination of service loadings from fatigue fracture surfaces. The method also allowed the identification of the load ratio R applied in laboratory tests and the load needed to cause fatigue crack growth, which can be inferred from fatigue fracture surfaces.
- The most important was to observe the good results from the load inference methodology from the postmortem fracture surface analysis.

References

1. T.L. Anderson, *Fracture Mechanics—Fundamentals and Applications*, 2nd ed., Boca Raton, CRC press, 1995
2. *ASM Handbook, Fatigue and Fracture*, Vol. 19, 1997, p 52–58
3. D. Broek, *Proceeding of the 2nd International Conference on Fracture*, Chapman and Hall, London, 1969, p 754
4. I. Nedbal, J. Siegl, and J. Kunz, Relation Between Striation Spacing and Fatigue Crack Growth Rate in Al-Alloy Sheets, *7th International Conference on Fracture (ICF7), Advances in Fracture Research*, Vol. 5, Pergamon Press, Huston, 1989, p 3483–3491
5. C. Masuda, A. Ohta, S. Nishijima, and E. e Sasaki, *Fatigue Striation in a Wide Range of Crack Propagation Rates up to 70 μm/cycle in a Ductile Structural Steel*, Fatigue Testing Division National Research Institute for Metals, 2-3-12, Nakameguro, Meguro-ku, Tokyo, Japan, 1980
6. Y. Murakami, N. Shiraishi, and K. Furukawa, Estimation of Service Loading From the Width and Height of Fatigue Striations of 2017-T4 Al Alloy, *Fatigue Fract. Eng. Mater. Struct.*, 1991, **14**(9), p 897–906
7. K. Furukawa, Y. Murakami, and S.-i. Nishid, A Method for Determining Stress Ratio of Fatigue Loading From the Width and Height of Striation, *Int. J. Fatigue*, 1998, **20**(7), p 509–516
8. SAE-AMS 4202C, *Aerospace Material Specification for Aluminum Alloy Plates*, The Engineering Society for Advancing Mobility Land Sea Air and Space, 2002
9. K. Furukawa, Method for Estimating Service Load from Striation Width and Height, *Mater. Sci. Eng. A*, 2000, **285**(1–2), p 80–84
10. M. Kikukawa, M. Jono, M. Adachi, Direct observation and mechanism of fatigue crack propagation *ATSM STP*, 1979, **675**, p 234–253